

# Estimation of stresses on 155mm artillery projectiles during launch phase using numerical simulations

Alan Catovic<sup>1</sup>, Faruk Razic<sup>2</sup>, Elvedin Kljuno<sup>3</sup>

<sup>1,2</sup> Defense Technology Department, Mechanical Engineering Faculty, University of Sarajevo, Bosnia

<sup>3</sup> Department of Mechanics, Mechanical Engineering Faculty, University of Sarajevo, Bosnia

---

## ABSTRACT

---

The paper provides an overview of research (analytical, numerical, and experimental methods) related to the stress state of artillery projectiles during movement through the barrel of the weapon. The characteristics of the 155mm HERA M549 and 155mm HE M795 projectiles, used in numerical simulations, are described. As a main goal of the research, numerical simulations were performed with the 155mm projectiles to determine the maximum equivalent stresses that occur during the launch of this ammunition. The obtained values were compared with the yield limit of the materials of the projectile components, in order to assess whether the plastic deformation would occur during the launch phase.

---

**Keywords:** high explosive projectiles, equivalent stresses, von Mises criterion

---

### *Corresponding Author:*

Alan Catovic  
Defense Technology Department  
University of Sarajevo  
Vilsonovo setaliste 9  
E-mail: catovic@mef.unsa.ba

---

## 1. Introduction

Generally, the state of stress on the projectile body can be defined by six following components:  $\sigma_x$ ,  $\sigma_y$ ,  $\sigma_z$ ,  $\tau_{xy}$ ,  $\tau_{yz}$  and  $\tau_{zx}$ , where a Cartesian coordinate system is usually used. Normal stresses are  $\sigma$ , and the shear stresses are  $\tau$ . The state of stress in a material can be formally written as a tensor (3x3 matrix). Shear stresses can be eliminated by rotating the coordinate system used to determine the stresses. The final three stresses are the principal stresses (normal stresses), and are designated as  $\sigma_1$ ,  $\sigma_2$ , and  $\sigma_3$ . Since the artillery projectiles are usually axially symmetric, it is convenient to use the polar-cylindrical coordinate frame, such that „ $x$ “ denotes the radial direction  $r$  from the axis of symmetry, „ $z$ “ denotes the symmetry axis direction, and „ $y$ “ denotes the circumferential direction (at the considered elementary volume), usually denoted by an angle „ $\theta$ “ in a polar-cylindrical coordinate frame. Von Mises, Tresca, and Coulomb are, generally, the three primary criteria for yield or material failure. When the component is formed out of metal, the von Mises or maximum distortion energy criterion is usually applied. It predicts that a hydrostatic state of stress would not lead to the failure of material and that the energy needed to alter the shape of the material is what yielding is caused by [1].

Based on knowledge of principal stresses and von Mises failure criteria, one can determine the equivalent stress. This is a scalar value that can be computed from the stress tensor. When the equivalent stress exceeds a yield strength, material begins to yield (plastic flow). When predicting the yielding of materials under complex loads, the equivalent stress is usually considered [1].

The stress state of a projectile can be determined using analytical and numerical methods. Different experimental methods can also be used, to predict relevant parameters during the gun launch phase, such as using the Aerofuze system, a projectile diagnostic telemeter for mortars and artillery [19]. Hard-wire telemetry can be used to measure the setback load on the projectile during the launch [22]. The use of

measurements and data telemetry in tests for analyzing projectile accelerations in the weapon is reported in reference [26]. Munition can be instrumented to describe gun-launch loads. One of the earliest scholars to instrumentally record the interior ballistics parameters was Lee [34]. Lee described seven 155 mm projectile firings with pressure sensors. Gun launch dynamics were characterized (displacement sensors, accelerometers) by Lodge and Dilkes [35].

A 120mm M832E1 HEAT round with instruments was analysed by Wilkerson and Palathingal [36]. Some of the commercial tools for determining accelerations in various directions were discussed by David et al [37]. A 120mm projectile's acceleration and pressures were obtained (data transmitted via telemetry) by Katulka et al. [38]. For a 4-in. air gun, Szymanski [39] devised an instrumentation kit comprising strain gages and accelerometers. The Picatinny Arsenal's Soft Catch Gun, which is used for projectile component testing, is described by Cordes et al. in [43].

Mission-critical components and safety-critical components are the two divisions that can be used for projectile parts. Every component is built with the premise that it must continue to function even under loads that are statistically predicted to be applied. Components that are essential to the mission are produced to withstand yielding. A structural member that could hurt a soldier or damage a gun is said to have a safety-critical component. Components that are necessary for safety must be tolerant to damage. For example, the projectile base and walls for the PG (precision guided) 155mm Excalibur projectile are safety-critical parts. Parts with low mass and confined parts are usually not safety-critical. The yield strength, ultimate tensile strength, elongation, and fracture toughness are typically included in the component specification for safety-critical parts. Three structural failure types are taken into account for a thorough analysis: yielding, buckling, and fracture [42]. In addition to loading of up to 5000 g at the muzzle, artillery projectiles experience axial loads of over 15000 g during the launch phase. The rate of spin for projectiles can reach 300 rev/s. A projectile may also be subject to off-axis loads from contacts with the gun tube walls brought on by balloting as it traverse the gun barrel [45].

This paper deals with von Mises yield criteria, and two conventional 155mm high explosive (HE) artillery projectiles will be considered (HERA M549 and HE M795) in FEM numerical analysis. Obtained maximum equivalent stress will be compared to the projectile body material yield strength and appropriate conclusions will be outlined.

In real-world military operations, the practical implications of these stress estimations are obvious since the projectile might explode prematurely inside the weapon barrel if inappropriately designed. So, determination of stresses on the projectile body in the initial phases of projectile design is important to alleviate mentioned problems since pressures during launch are very high, with accelerations reaching 40000g.

## 2. Review of literature

Carlucci [1] gives an introduction to projectile analytical structural analysis (methods) during the launch phase of a projectile. He gives formulas for longitudinal, hoop and radial stresses for several characteristic projectile body sections and describes their origin (external pressure, setback force, rotation of projectile, rotating band engraving force, mutual interaction of explosive and body).

Carlucci also gives an introduction to interior ballistics calculations, needed to provide values of base pressures (from propellant gas) and acceleration of a projectile in the barrel of the weapon (these values can then be used in the analytical and numerical analysis of stresses in projectile during the launch phase).

Krier and Summerfield [2] provide a review of interior ballistics models and different types of gun propellants in use. Theoretical aspects of interior ballistics of guns are also covered in Engineering Design Handbook (AMCP 706-150) [3], where appropriate experimental methods are also reviewed.

ARDEC (Armament, Research, Development and Engineering Center) researchers measured the explosive base pressure for projectiles during launch. They concluded that lubricated cases with charge castings had pressures in the order of 10% to 20% of base pressures from the propellant gasses, whereas good explosive charge castings had pressures in the order of 7% to 16% of the base pressure. Explosive charge defects (such as voids, small fractures, cracks, porosity, and cavities) are significant since they serve as locations for stress concentrations that can cause localized heating, the formation of hot spots, and igniting [7,8].

To determine if explosives are suitable for gun launch, Baker and Swaszek [7,8] gave an overview of in-bore parameters for different weapon systems (Table 1) and experimental setback actuators. The pressure in an explosive charge is lower than the applied pressure of propellant gases to the projectile base (due to the explosive being loaded by projectile acceleration rather than propellant gases).

Table 1 Generic data for acceleration and pressure for different weapon systems [7]

Weapon system	Projectile accelerations ( $\cdot 10^3$ g)	Chamber pressure (MPa)
Artillery	4-30	70-500
Mortars	1-13	20-140
Tank Guns	25-120	200-830
Medium Caliber weapon	50-200	140-1400

Djordjevac [9] conducted a theoretical analysis of stress distribution inside the body of an artillery projectile (105mm, HE, M1), during its movement through the weapon barrel. He also performed numerical analysis using the Finite Element Method (FEM), and the results obtained by the FEM and by the classical method are compared. It was concluded that numerical analysis is an adequate tool for assessing the stresses on the projectile body. It is computer resource more intensive but gives clearer picture of overall stress state in different part of projectile (suitable for complex geometries).

Stiefel [13] reviews the structural design of projectile (including FEM analysis), thermodynamic properties of military gun propellants, gun barrel erosion, base bleed systems for projectiles, and provides pressure-velocity-time-travel curves for different ammunition types (Figs 1-4 represent interior ballistics curves for 155mm high-explosive projectiles, presented in [13]).

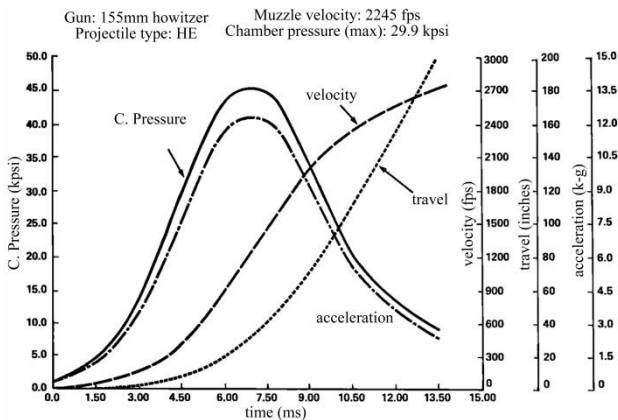


Fig. 1 Pressure, velocity, acceleration, travel vs time for a HE round fired with a high-zone charge from a 155mm howitzer [13]

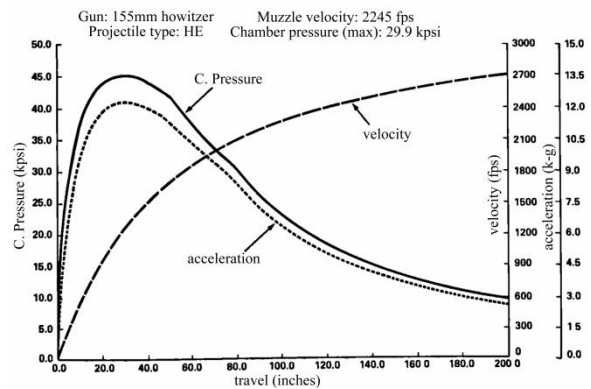


Fig. 2 Pressure, velocity, acceleration vs travel for a HE round fired with a high-zone charge from a 155mm howitzer [13]

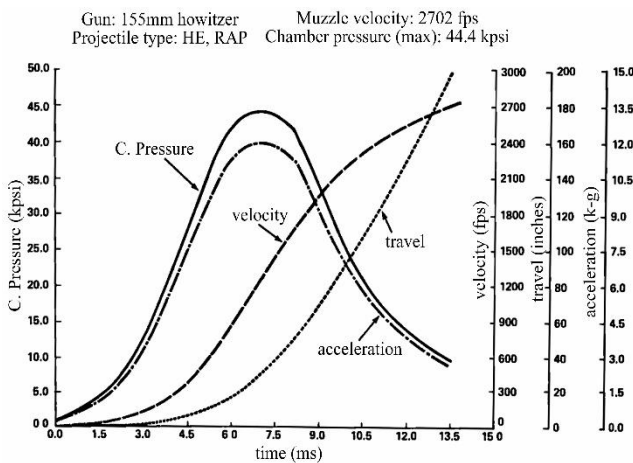


Fig. 3 Pressure, velocity, acceleration, travel vs time for a HERA round fired with a high-zone charge from a 155mm howitzer [13]

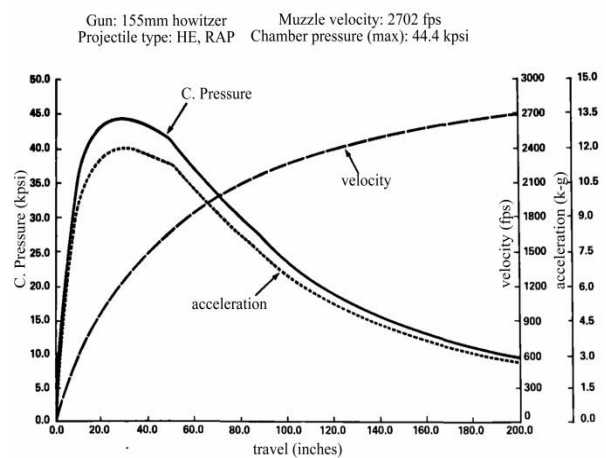


Fig. 4 Pressure, velocity, acceleration vs travel for a HERA round fired with a high-zone charge from a 155mm howitzer [13]

To give a idea of how typical artillery systems function, Tangay [10] calculated muzzle velocity and peak acceleration of projectiles weighing between 10 and 50 kg in a variety of artillery gun systems, utilizing a variety of propellants. It is found that muzzle velocity and peak acceleration decrease with increasing projectile mass. It is also found that the extended (52-caliber) guns produce higher muzzle velocity than the guns in service and that all 155 mm guns outperform the 105 mm guns.

Mulherin et al. [18] explored the fracture mechanics to define critical defect sizes in the 155mm, HE, M107 projectile body, made of isothermally processed HF-1 steel. Critical crack sizes are calculated for each of the main sources of stress (i.e. encountered during rough handling and launch). Also, experimental (estimation of compressibility of Comp. B and strain gage tests for prediction of engraving forces) and numerical simulations of stress were performed. The effectiveness of the method is examined through drop testing using projectiles that have been purposefully pre-flawed. They concluded there are two parts of projectile where care has to be taken for safe structural integrity. These are the interior part under the rotating band and the front ogive region of the projectile, where even very small longitudinal cracks could be critical [18].

Taylor et al.'s [20] estimation of the explosives' sensitivity to premature ignition during an artillery projectile's launch was based on experiments. Compression alone, rapid compression heating the air trapped next to the explosive, and frictional heating were the ignition methods taken into consideration [20]. The stress of a gun barrel during the launch was investigated by Babei et al [23].

Ray et al. [25] examined the dynamic response of a projectile to gun chamber pressure dynamics produced by a densely packed propellant charge during the launch. The Army's interior ballistics code ARL-NGEN3 was used to start the modeling process since it estimates the solid propellant charge's ignition, flame spread and combustion. The projectile's reaction to the pressure dynamics was then modeled using the EPIC [25].

The behavior of the leak flow during a launch was predicted by Fredriksson [27] using a CFD model. To account for the projectile's motion, RANS-model and a dynamic mesh have been used.

Wilkerson et al. [28] employed a transient FEM model to simulate the 155-mm SADARM Projectile's launch environment. Due of the sensitive electronic components in projectiles like SADARM, careful consideration must be given when analyzing the structural package. These projectiles, as well as PGM (precision guided munition), require sturdy designs that can withstand high accelerations and spin rates.

The Excalibur 155-mm artillery projectile's four-axis canard actuation system (CAS) was studied by Bender [29], using FEM. In order to determine whether CAS can withstand the harsh launch environment of high-performance 155-mm howitzers and still perform as intended, its structural robustness was evaluated.

Verberne [41] conducted a comprehensive explicit axisymmetric Lagrangian-Eulerian multiphysics finite element analysis of the launch process of precision guided projectiles (including coupling and interaction effects). Additionally, Verberne [30] performed a nonlinear dynamic FEM analysis of the cannon launch process to ascertain the underlying mechanisms relating to solid-solid interaction between precision guided projectile and the inner walls of the barrel.

Dohrn et al.'s evaluation of the most recent methods for estimating gun launch dynamics parameters may be found in [31]. Lagrangian hydrocodes, short duration explicit codes, commercial/governmental codes, a thorough grasp of physics, high fidelity experimentation, and knowledge of what phenomena occurs within a gun are some examples of methods used.

According to Chen [32], on-board electronics for precision projectiles must be able to withstand pressure waves that most propelling charges experience during their early combustion phase as a result of pressure imbalance in the chamber. A deterministic transient stimulation followed by a stochastic method was used to model pressure waves.

Excalibur, a 155mm precision guided projectile, was test-fired with a variety of propellant charges while it was being developed. The reliability, structural integrity, and performance of various charges were tested, according to Cordes et al.'s report [33]. The accelerations and pressures from several tests with various propellant charges are also compiled in their research. For the majority of experiments, gun barrel pressures and on-board accelerations were obtained.

Ball [40] analytically examined the structural integrity of the motor case of a 127mm gun launched projectile as a function of case thickness and maximum launch acceleration.

An FEM model was created by Chakka et al. [45] to describe how a projectile interacts with the gun barrel in launch phase. In order to lessen transmitted shocks during the projectile launch, they also looked at the usage of composite plates (carbon fibers in an epoxy matrix) to support electronic payload.

Alexander [46] investigated interaction of the barrel and the projectile in the weapon barrel, as well as the projectile's exit tip-off parameters, using Abaqus program (FEM method).

Petersen [47] suggested a test method to collect data on the dynamics of the 155mm Advanced Gun System barrel as a projectile moves down the gun tube to support modeling initiatives using sensors on the gun barrel to monitor the location, acceleration, and strain during firing. Data collected is compared to barrel-projectile interaction (FEM)

### 3. Description of 155mm HE projectiles

#### 3.1 Projectile 155mm, HERA, M549

The 155mm M549 (Fig. 5) is an extended range, high explosive rocket assisted (HERA) projectile for use in long-range harassment and interdiction fire missions. It is used as a blast effect and fragmentation projector against personnel and materiel. It has a mass of 43,6 kg (with fuze) and max. length of 874 mm (with fuze), and consists of two main components, a warhead with 6,8 kg of TNT (M549A1), and a solid propellant rocket motor. Model M549 is filled with 7,3 kg of Composition B. Components are connected with threads so that the projectile surface is streamlined. The ogive cavity has been fitted with a supplementary charge. Solid rocket propellants (2,9 kg) are placed in two segmented grains inside the rocket motor body. An ignition cap is included in each of the grain's segments. The boat tail rocket motor base of the projectile has a recessed motor nozzle in the center, and thrust is directed along the axis [4,16].

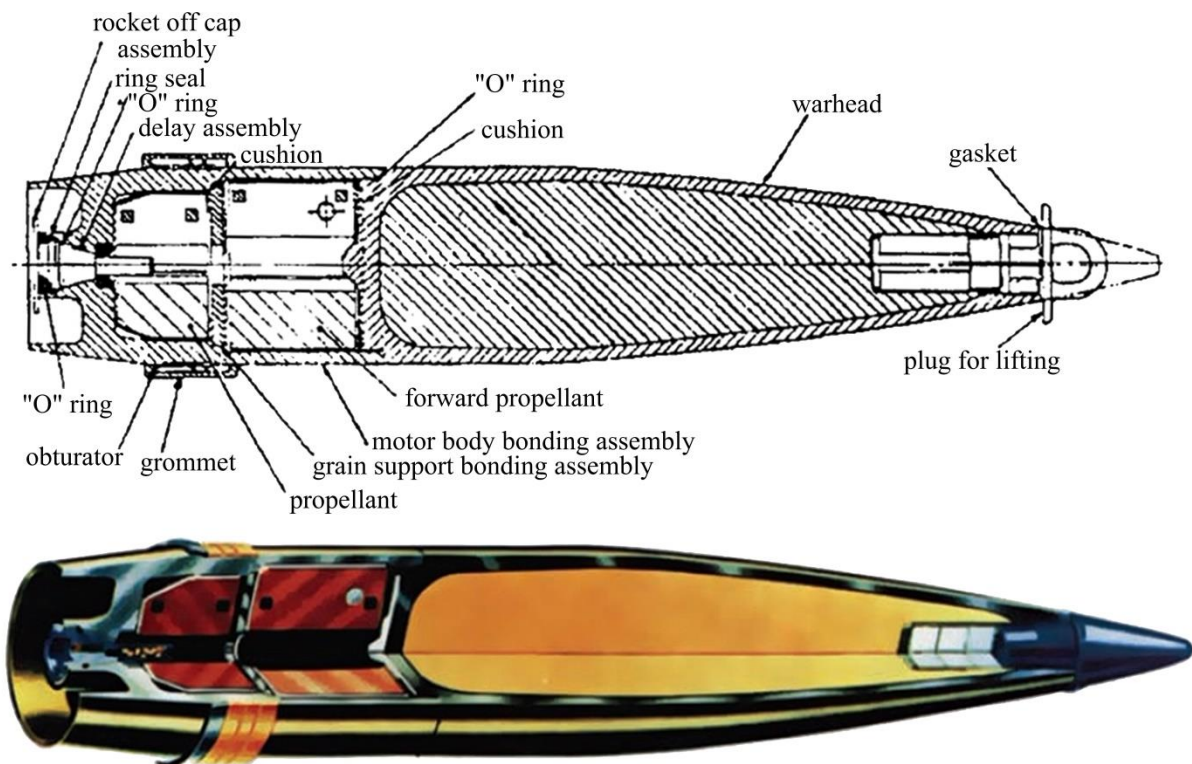


Fig. 5 Artillery projectile 155mm, HERA, M594 [4,16]

The rotating band engraves in the barrel rifling when the weapon is fired, providing the projectile with gyroscopic stability. To stop propellant gases from escaping from behind the projectile, the obturator and rotating band create a seal. The projectile is propelled through the barrel at the proper velocity by rapidly expanding gases. The delay charge burns for around 7 s after the projectile is launched, at which point the rocket propellant ignites (burning time is 3 seconds), which increases the velocity and the range.

Fuzes for 155mm munition are: PD (M557, M78 series, M739 series, MK399 MOD 1, MTSQ: M564, M582 series), Prox. (M728, M732 series), ET (M767). In US Army it can be used on towed howitzers M114, M198,

M777, and on SPH M109 [4,16]. Because the rocket motor could fail to ignite, a 6 km safety zone is needed (in front of the target).

The fact that this projectile is produced from an alloy steel rocket motor body and a thin-walled, long ogive, high-fragmentation steel (HF-1) warhead best demonstrates the state of the art in metal parts manufacturing technology. MIL-S-50783 specifies the chemistry, deoxidation procedure, steel melting method, and warhead body materials.

The M549 projectile may travel 30 kilometers when fired from 155mm weapons with several propelling charges. As a result, when inside the gun tube, the warhead is subject to various degrees of spin, setback, muzzle velocity, and chamber pressure. It must also be able to effectively fragment when its explosive charge is detonated, in addition to properly withstanding these mechanical loads without deforming during the launch phase. The shape, mass, moments of inertia, and center of gravity required to satisfy interior, exterior, and terminal ballistic criteria determine the mechanical properties of the warhead body. The ratio of the high-explosive charge to the warhead body mass, the steel's chemical composition, and heat treatment all affect how the warhead body fragments. Prior to the M549's introduction into production with the new high-fragmentation steel, significant studies were conducted on steel mill operations, steel chemistry, forging operation optimization, multi-parting technique evaluation, forging spheroidized annealing, heat treatment, machine tool materials, and machineability.

A nozzle is located on the motor body's spin axis. It is comprised of an alloy of high-strength steel (AISI 4340). Hot forging, heat treating, and machining is the most practical method for creating the rocket motor body for this projectile because it is compatible with shaping and machining 4340 steel and can meet the minimum yield strength requirement (1241 MPa, with minimum elongation of 10%). It is possible to apply rotating bands with welded overlays that have a thick enough underside to withstand chamber pressure and engraving forces. The motor body needs to be stress relieved or heat treated after the welded overlay has been applied. Prior to heat treatment, the body must be carefully machined to prevent sharp edges, surface imperfections, and sudden geometric changes. Cordes et al [42] report on data for 4340 steel (for 66 specimen, average yield strength was 1501,6 MPa, and tensile strength 1861,4 MPa), used in 155mm Excalibur PG projectile.

High-fragmentation steels are considered ones that, due to their structure and characteristics, produce appropriate fragmentation effects to a particular target. Antimaterial or antipersonnel applications are both possible. Many carbon and alloy steels, mostly those with medium-to high-carbon contents, were examined so far (heat treatment method, warm-working, hot-working, cold-working). After that, the projectile configurations of the most promising possibilities were produced, and they underwent Pit fragmentation testing. The results are compared with the original fragmentation material, pearlitic malleable iron. Arena testing was done on the select few successful candidates to identify velocity and fragment dispersion patterns for a lethality assessment. AISI 52100, AISI 1340, and HF-1 were those that were approved following evaluation over a number of years. These three steels, which were authorized in the order specified [5,16], have been utilized to create projectiles on assembly lines. Table 2 lists the chemical composition of high-fragmentation steels.

Table 2 Chemical composition of high-fragmentation steels [5]

Steels	C, %	Mn, %	P, %	S, %	Si, %	Cr, %
52100	0,95-1,10	0,25-0,45	0,025	0,025	0,15-0,30	1,30-1,60
1340	0,38-0,43	1,60-1,90	0,035	0,040	0,15-0,30	-
HF-1	1,00-1,15	1,60-1,90	0,035	0,040	0,70-1,00	-

The 152mm M409 HEAT-T-MP projectiles were made using the bearing steel 52100 (table 2). There were several issues with this application of steel, including temperature controls that were too restrictive, so 52100 steel is no longer applied for projectile manufacturing.

For the high-fragmentation steel 1340 (manganese alloy; table 2), warm-working, hot cup-cold draw, and hot forge-heat treat applications have all been involved in its utilization. It has been employed with mechanical characteristics ranging from 552 MPa to more than 965 MPa.

The 155mm HERA M549, 155mm HE M795, 203mm HERA M650 projectile bodies are manufactured from HF-1 steel. The yield strength required for HF-1 steel is 965 MPa, with 5% min. elongation [5].

### 3.2 Projectile 155mm, HE, M795

The 155mm, HE, M795 (Fig. 6) projectile belongs to a new group of ammunition for 155mm howitzers that has a comparable ballistics. Eventually, it will take the place of the 155mm, HE, M107 projectile. The M795 projectile is used to provide division/corps units with conventional support.

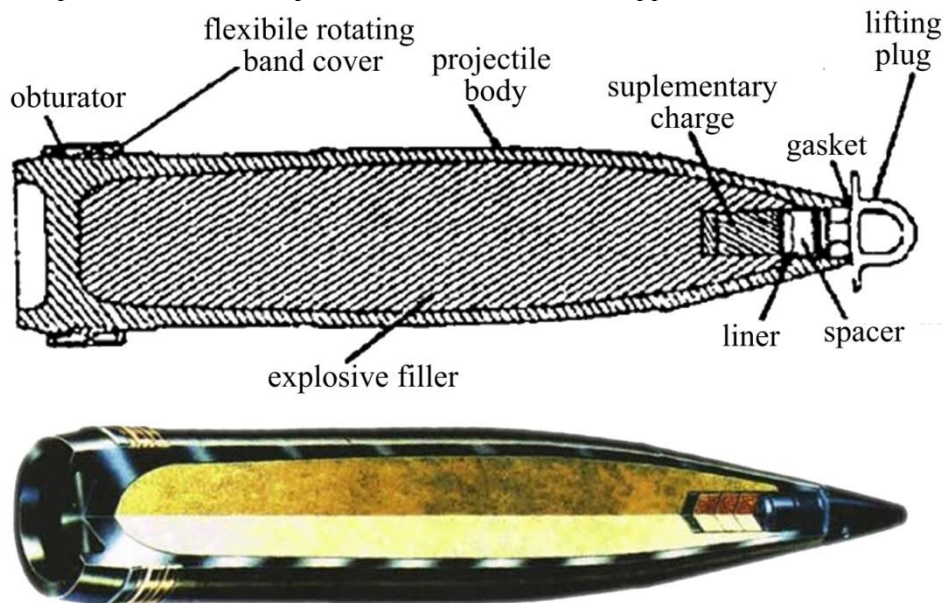


Fig. 6 Artillery projectile 155mm, HE, M795 [4,17]

The M795 projectile can also serve as a registration round for the M483A1 family of cargo projectiles because it is ballistically comparable to them, despite being 50mm shorter. Length of projectile with fuze is 843 mm and total mass is 46,7 kg. Around 10,8 kg of TNT or IMX-101 explosive is inserted into the body assembly of the M795 projectile [24]. The IMX-101 charge increases handling safety by reducing vulnerability to accidental munition explosions. Projectile has hollow base boat tail (HB BT) design rear side. The high fragmentation steel (HF-1) body has a rotating band of gilding metal close to the base. The 155mm M107's swaged rotating band is replaced by a welded band on the M795 in order to fire propelling charges M119 or M203, extending the projectile's range. The rotating band's obturator is made of plastic. The projectile is equipped with a flexible rotating band cover that shields it during shipping and handling, as well as a protective lifting plug at the projectile's frontal part. The projectile uses (short intrusion) proximity fuzes, mechanical time, and impact fuzes.

Maximum range of projectile 155mm HE M795 is up to 22,5 km and it has increased accuracy due to better aerodynamic shape (comparing to older 155mm HE projectile models). CEP of M795 is 139 m at max. range (with 39 caliber weapon). This projectile increases the range of 155mm HE M107 projectile for around 28,5%.

Additionally, M795 offers an 80% increase in lethality comparing to projectile 155mm, HE, M107 against trucks and almost 100% increase against soldiers on the battlefield. A two-directional Course Correcting Fuze (CCF) that uses GPS, offering better accuracy, can be added to the projectile M795.

Designers are currently attempting to enhance ballistic performance and incorporate a better drag reduction system based on the successful 155mm M864 Extended Range DPICM BB Projectile, using the production M795 projectile as a baseline. Known as the M795E1, this projectile should maintain its extended range capability (28,7-37 km) to counter the longer range artillery threat posed by potential adversaries while offering a significantly larger HE charge, high fragmentation warhead, and improved lethality over the M549A1 HERA projectile [4,16,17].

Brady and Goethals [6] suggest that the 155mm M795 and M549A1 projectiles are better munition options for large area targets, while the PGP 155mm Excalibur M982 was found to be best suited for engaging point and small area targets of higher value.

Weapons used in US Army with this projectile are mainly SPH M109, and towed howitzers M198 and M777. General description of 155mm howitzers can be found in [21].

## 4. Numerical simulations of 155mm conventional artillery projectiles during the launch phase

### 4.1 Transient dynamic analysis

Numerical simulations performed in the research were done in the Transient Structural module, a component of the ANSYS Workbench system. Workbench environment provides overarching integration with CAD and process of design. Applications in the Transient Structural module used in the research include: Engineering, Geometry Modeler, and Mechanical. Analysis types available in Mechanical are: structural (static/ transient), and linear/nonlinear structural [14]. Fig. 7 shows the generic procedure used in numerical simulations.

- **Preliminary Decisions**
  - **What type of analysis: Static, transient, modal, etc.**
  - **What to model: Part or Assembly?**
  - **Which elements: Surface or Solid Bodies?**
- **Preprocessing**
  - **Attach the model geometry**
  - **Define and assign material properties to parts**
  - **Mesh the geometry**
  - **Apply loads and supports**
  - **Request results**
- **Solve the Model**
- **Postprocessing**
  - **Review results**
  - **Check the validity of the solution**

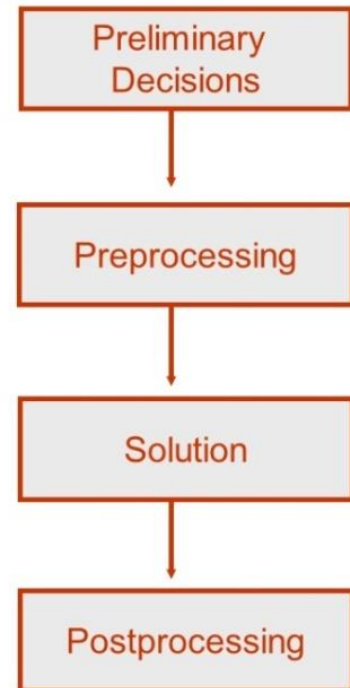


Fig. 7 Basic procedure in numerical simulations [14]

A technique used to assess a structure's dynamic reaction to any kind of time-dependent stress is transient dynamic analysis, often known as time-history analysis. When a structure is subjected to any combination of static, transient, and harmonic loads, this kind of analysis can be used to identify the time-varying displacements, strains, stresses, and forces that the structure experiences. Because of how quickly the loading occurs, inertia or damping effects are thought to be significant [15].

A transient dynamic analysis is used to solve following equation of motion: [15]

$$(M)\{\ddot{u}\} + (C)\{\dot{u}\} + (K)\{u\} = \{F(t)\} \quad (1)$$

Here (M) is mass matrix,  $\{\ddot{u}\}$  is nodal acceleration vector, (C) is damping matrix,  $\{\dot{u}\}$  is nodal velocity vector, (K) is stiffness matrix,  $\{u\}$  is nodal displacement vector, and  $\{F(t)\}$  is defined as load vector.

Three methods are available for solving Equation (1) [48]:

- Central difference time integration method - used for explicit transient analyses only.
- Newmark time integration method - used for implicit transient analyses (one of the most popular time integration methods as a single step algorithm).
- HHT time integration method - used also for implicit transient analyses. This method is an extension of the Newmark time integration method.

Equation (1) can be viewed as a collection of "static" equilibrium equations that also account for damping forces (C) and inertia forces (M) at any given time  $t$ . The integration time step is the amount of time that separates subsequent time points. Because it typically requires more computer resources and "engineering" time than a static study, transient dynamic analyses are more complex than static analyses. The structural

dynamics problems concerned with the mechanical behavior governed by the differential equation (a) can be classified into two classes: linear and nonlinear problems.

In linear structural dynamics systems, the internal load is linearly proportional to the nodal displacement, and the structural stiffness matrix remains constant. Therefore, Equation (1) can be rewritten as [48]:

$$(M)\{\ddot{u}_{n+1}\} + (C)\{\dot{u}_{n+1}\} + (K)\{u\} = \{F^a(t)\} \quad (2)$$

where (K) is structural stiffness matrix. Among direct time integration methods for numerically solving the finite element semi-discrete equation of motion given in Equation (2), several methods such as the Newmark method and the generalized method (Chung and Hulbert) are incorporated in the program.

As the generalized- method recovers the Wood-Bosak-Zienkiewicz method (also called WBZ- method) (Wood et al.), the Hilber-Hughes-Taylor method (also called HHT- method) (Hilber et al.), and the Newmark family of time integration algorithms, the Ansys program allows you to take advantage of any of the these methods by specifying different input parameters. More details on these equations and time integration algorithms is available in [48].

#### 4.2 Verification of numerical model

The verification of the numerical model used was done on the model of the 105mm HE M1 projectile, in order to compare the results (maximum equivalent stress; von Mises yield condition used) with the results of other authors [9].

The steps in the numerical simulation to verify the numerical model were as follows:

- create a 2D model of the projectile in CAD software, based on the projectile dimensions.
- Create a 3D projectile model with a half section in CAD software (rotation of the 2D model by 180° around the longitudinal axis). A half-section is used to reduce the mesh and simulation run time.
- Export the resulting 3D projectile model as an .igs file type in CAD software.
- Use the Transient structural module (transient analysis) in Ansys software.
- Define the materials of the projectile components. The materials for this case (verification procedure) were modeled as in reference [9]. The fuze is not modeled in CAD - in this case its effect was replaced by the dynamic pressure curve that is created due to the mass of the fuze and the acceleration of the projectile.
- Insert the 3D projectile model into the Geometry modeler in Ansys and add materials to the projectile components.
- Insert the mesh into the numerical model in the Mechanical module within Ansys. The mesh consisted of tetrahedral elements because they are suited for the irregular geometry.
- Add boundary conditions, in this case load (pressure). In our analysis, we took into account the real pressure change P(t) on the bottom of the projectile, as well as P(t) curve created by the fuze (because of inertia during movement due to the acceleration of the projectile and mass of fuze). The pressures were taken on the basis of the interior ballistics parameter calculation for the 105mm HE M1 projectile, available also in [9]. These data (for pressure load) are tabulated for use in Ansys calculations.
- An additional boundary condition is axial symmetry, where the central surfaces of the 3D model are selected and the Symmetry condition is added to them (axis normal to these surfaces must also be defined).
- Perform a simulation in Ansys, with a total analysis time of 9.8 ms, which corresponds to the time the projectile spends in the barrel (internal ballistics calculation). The duration of the simulation depends also on the numerical mesh and the characteristics of the computer, but it is significantly shorter than if a full 3D numerical model were used.

Results obtained in numerical simulations (Figs. 8, 9 and 10) agree well with the results of other authors research [9]. In reference [9], the maximum equivalent stress obtained by numerical simulation varies from 530-560 MPa (the author performed several types of numerical analyses).

In our case, the maximum equivalent stress was about 533 MPa (Fig. 8), which is a satisfactory matching of the results. Accordingly, we can use this numerical method for the calculation of equivalent stresses on other projectiles.

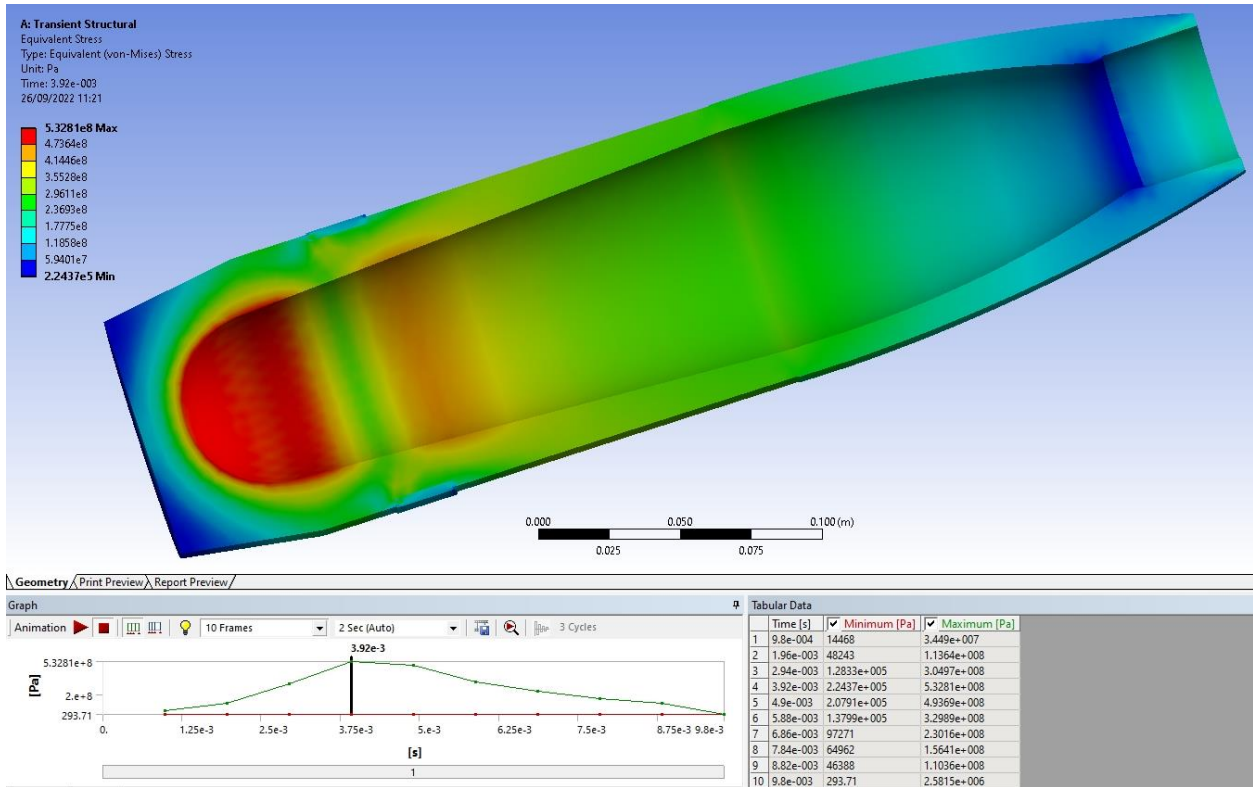


Fig. 8 Equivalent stresses (von Mises condition) for 105mm HE M1 projectile (verification of numerical model)

Fig. 9 shows equivalent stresses 105mm, HE, M1 projectile with explosive charge present, and Fig. 10 shows equivalent stresses on outer side of projectile body. Stresses on explosive charge are under 50 MPa.

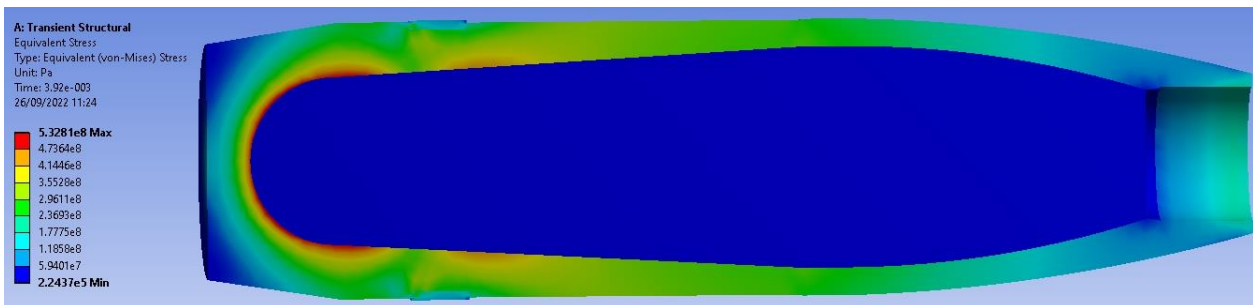


Fig. 9 Equivalent stresses on 105mm HE M1 projectile with explosive charge present

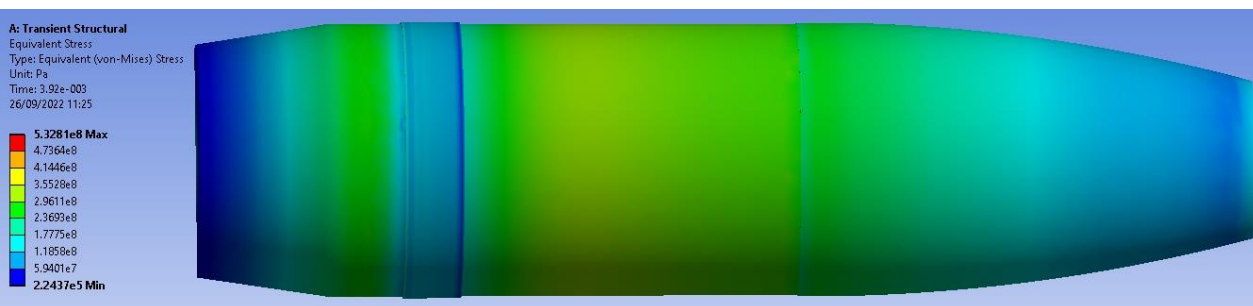


Fig. 10 Equivalent stresses on outer side of 105mm HE M1 projectile

### 4.3 Numerical simulations of 155mm HE projectiles and results analysis

As a main goal in the research, numerical simulations in Ansys Transient Structural module were conducted to estimate the equivalent stresses on artillery projectiles 155mm HERA M549, and 155mm HE M795. Calculations were performed to simulate the launch conditions of these projectiles. In analysis, the rotation of the projectiles was not taken into account (generally, axial stresses are dominant during the launch of

projectiles [1,9]). A supplementary charge in the frontal projectile cavity is approximated as a part of an explosive charge (this part of the projectile is not critical regarding the equivalent stresses). Fuze mass is taken into account using the data for projectile acceleration, fuze mass, and frontal cross-section of the projectile body. This is, generally, more accurate than using the real fuze geometry and material data in simulation since fuze is assembled out of many components made from different materials. CAD models of these projectiles were made using publicly available drawings (drawings with all dimensions were not available so small errors compared to real geometry are possible), and are presented in Fig. 11 (models represented in scale).

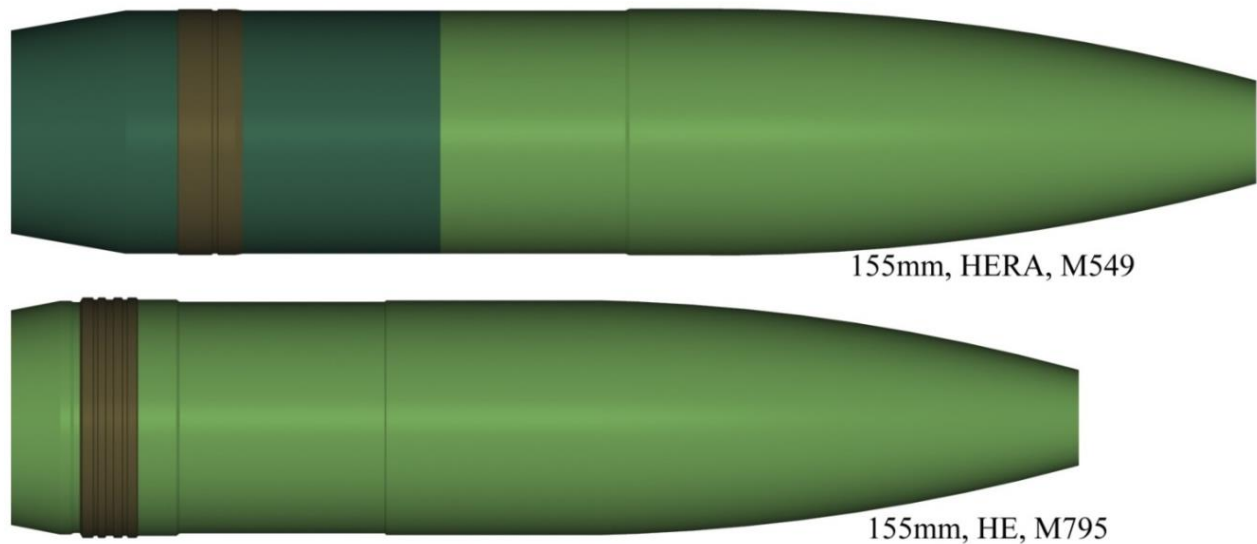


Fig. 11 CAD models of 155mm projectiles, HERA M549 and HE M795 (models in scale)

Materials used in simulations are characterized (from different literature sources) as presented in table 3. Data for rocket propellant, used in projectile M549 are classified, so available mechanical characteristics data for generic solid rocket propellant were used.

Table 3 Characterization of materials used in numerical simulations [9,11,12]

Material	Material	Density (g/cm <sup>3</sup> )	Elastic modulus (Pa)	Poisson coefficient
Rocket motor	AISI 4340	7,85	$2 \cdot 10^{11}$	0,3
Projectile body	HF-1 steel	8,00	$2 \cdot 10^{11}$	0,3
Rotating band	Gilding metal	8,88	$1,15 \cdot 10^{11}$	0,33
Explosive charge	TNT	1,55	$2,55 \cdot 10^9$	0,39
Explosive charge	Composition B	1,65	$3,72 \cdot 10^9$	0,36
Rocket propellant	-	1,60	$1,5 \cdot 10^7$	0,4

Numerical meshes for given projectile models are shown in Fig. 12. In the simulations, 574945 tetrahedral elements were used for projectile 155mm HERA M549, and 513455 elements for 155mm HE M795 projectile. A larger number of elements greatly increases simulation time and results don't change significantly. For these meshes, simulation time was in the order of 3h on CPU AMD Ryzen 7 (8 processors, distributed parallel processing).

Loading pressures on projectile base for given projectiles are defined (in tabulated form; transient dynamic analysis) in Ansys using an interior ballistics data for howitzer M198 (M203 charge). In numerical analysis, the real pressure curves  $P(t)$  on the projectiles base, as well as pressures created by the fuze (setback during movement due to the projectiles acceleration and mass of fuze) were taken into account. The fuze used was standard PD M557 model with a mass of 0,975 kg. Sectional areas of the frontal part of the projectile body (needed for calculation of fuze pressure on the body) were determined from the drawings. Projectiles acceleration data were also acquired from an interior ballistics solution. Interior ballistics data for 155mm projectiles (and several other types of projectiles) can be found in [13,44].

Equivalent stresses obtained for projectile **155mm HERA M549** are presented in Fig. 13 (for maximum pressures). Probes with stresses values are inserted into the results to better visualize obtained data (variation of stresses on different parts of projectile). In the lower part of Fig. 13, a diagram of maximum equivalent stresses is presented as a function of time. It can be seen that the largest equivalent stresses (1340,9 MPa) are

present in the rocket motor body. This part of the projectile is made from AISI 4340 steel with a min. requirement of 1241 MPa for yield strength, and min. elongation of 10% [5]. Carlucci et al [42] report on the average yield strength of 1501,6 MPa, and tensile strength of 1861,4 MPa, for steel 4340, used in 155mm Excalibur PG projectile.

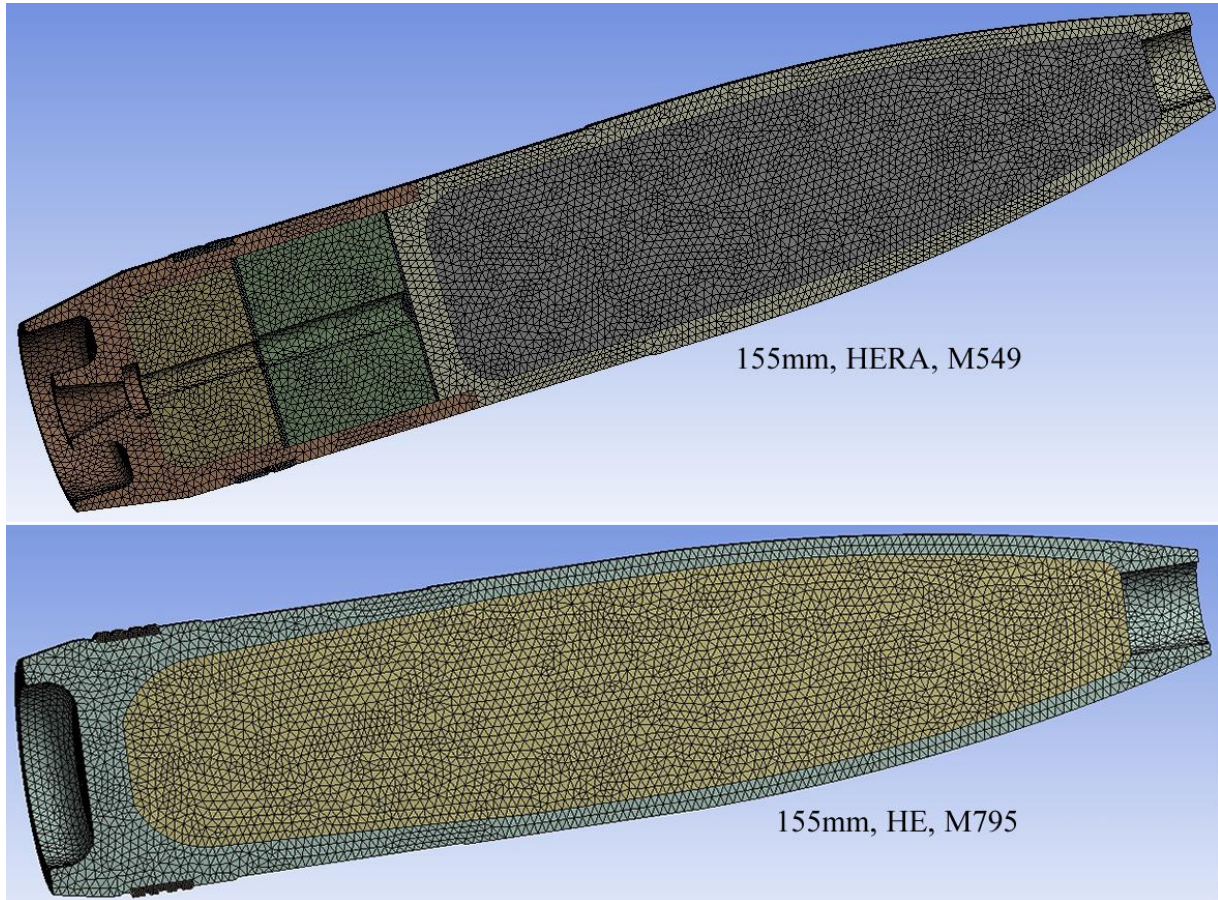


Fig. 12 Numerical meshes for projectiles 155mm HERA M549 and 155mm HE M795

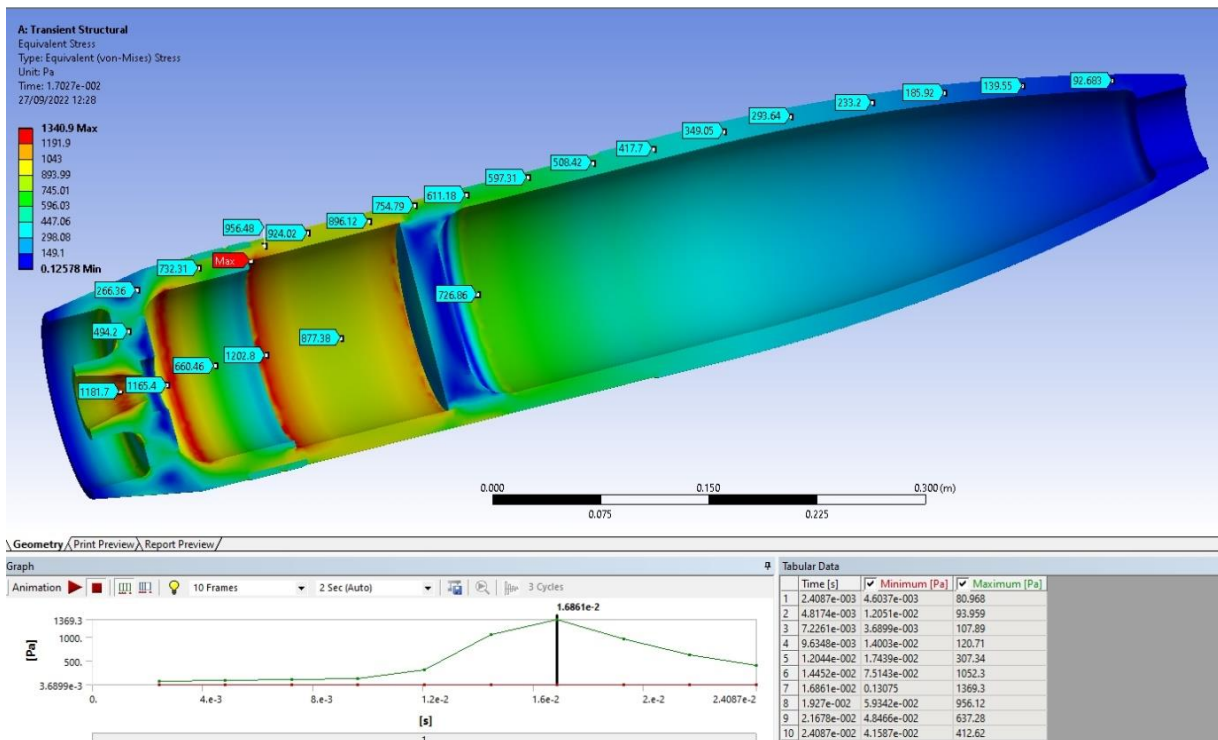


Fig. 13 Equivalent stresses for projectile 155mm HERA M549 (warhead and rocket motor body)

Taking into account data from reference [42], and since the maximum equivalent stress obtained by numerical simulation is around 1340 MPa, one can conclude that no plastic deformation will occur on any segment of the rocket motor body. The critical section on the rocket motor is the segment of the body next to the upper rocket propellant, on the section below the rotating ring (Figure 13), a result which is in accordance with the conclusions from the reference [18]. At the base of the rocket motor, next to the lower rocket propellant, there is also a section with an increased value of the equivalent stress (fig. 13). Large values of equivalent stresses are also present in the nozzle (inner part) of the rocket motor.

Regarding the warhead body, made from steel HF-1, Fig. 13 shows that maximum equivalent stresses are less than 750 MPa. Since the mechanical properties of steel HF-1 required are yield strength of 965 MPa and 5% min. elongation [5], obtained results show that the warhead body will not undergo plastic deformation during the launch from this weapon (howitzer M198).

In fact, in this case, the warhead body can even be designed thinner to accommodate more explosive charge which can result in the increase of fragment velocity. This can potentially reduce the mass and number of fragments, so a terminal ballistics optimization study (fragmentation effects) should also be performed.

Fig. 14 shows equivalent stresses for 155mm HERA M549 projectile, with explosive charge and rocket propellant present. It can be seen that stresses on explosive charge and rocket propellant are lower than 100 MPa. Generally, for explosive safety during the launch, the most important characteristic is absence of any defects: voids, cracks, porosities and cavities etc.

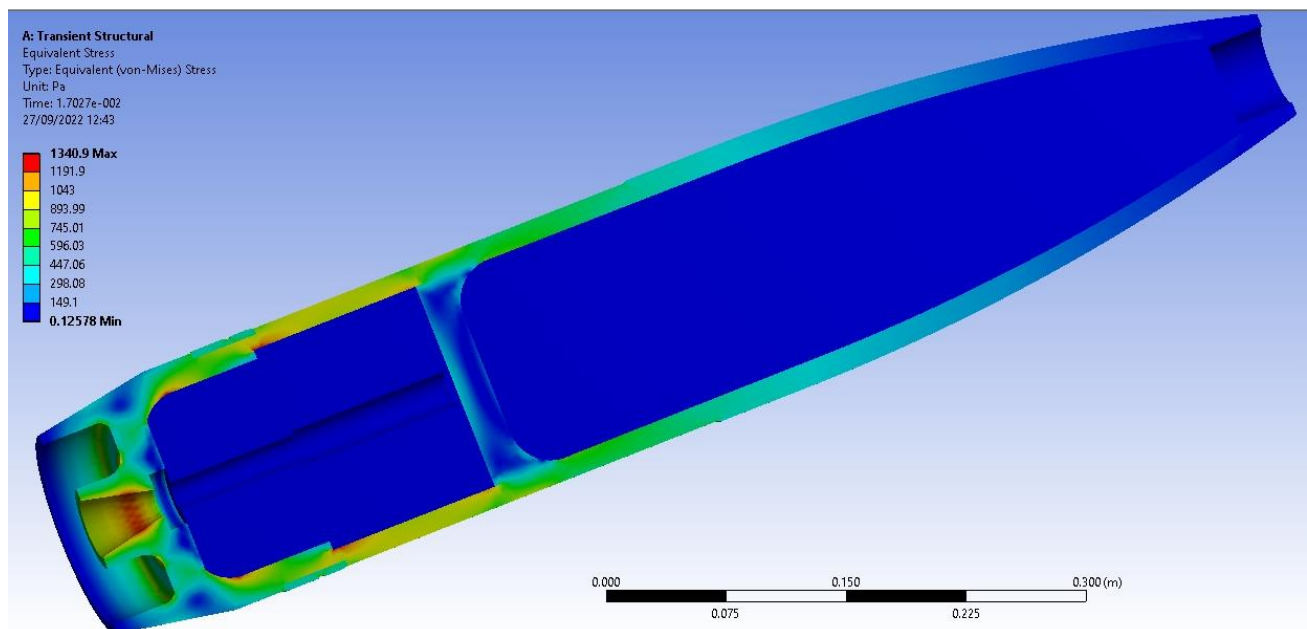


Fig. 14 Equivalent stresses for 155mm HERA M549 projectile (all components)

Fig. 15 shows equivalent stresses for 155mm HERA M549 on the outer part of the projectile. As one moves towards the end of the projectile, in this case, the equivalent stresses increase, except in the rocket motor body's outer part (behind the rotating band), where the stresses decrease.

Results of numerical simulation (equivalent stresses) for artillery projectile **155mm HE M795** are presented in Fig. 16 (for maximum pressures). Probes with stress values are also inserted into the results (stresses contours).

As can be seen in Fig. 16, in this case, the stresses on the projectile body are somewhat higher than in the case of the 155mm HERA M549 projectile body. At the base part of the projectile (in contact with the explosive), below the rotating band, there is a location with the highest equivalent stress value (926,4 MPa). In this case too, the stress is the highest under the rotating band, as a combination of the reduction of the cross-section of the projectile body and the cumulative mass of the projectile and fuze in front of the given section.

The obtained values of the equivalent stress are nevertheless still lower than the yield limit of the projectile material (HF-1), which is 965 MPa, so even in this case, there will be no plastic deformation of the projectile body during movement through the barrel of the weapon (howitzer M198).

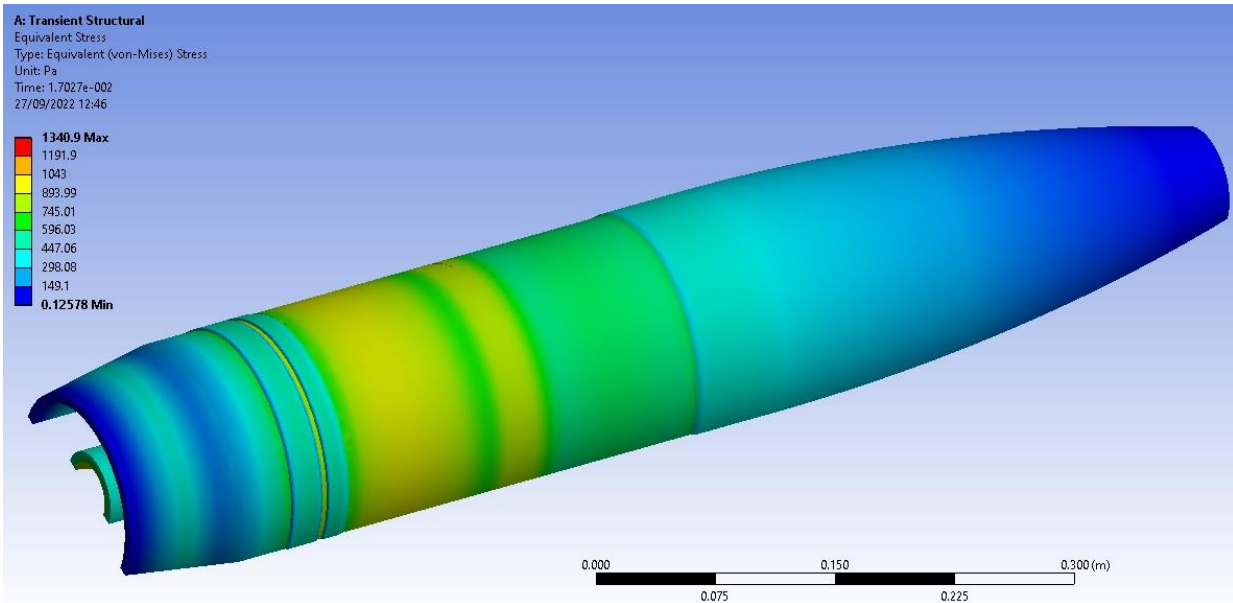


Fig. 15 Equivalent stresses for 155mm HERA M549 on the outer part of projectile

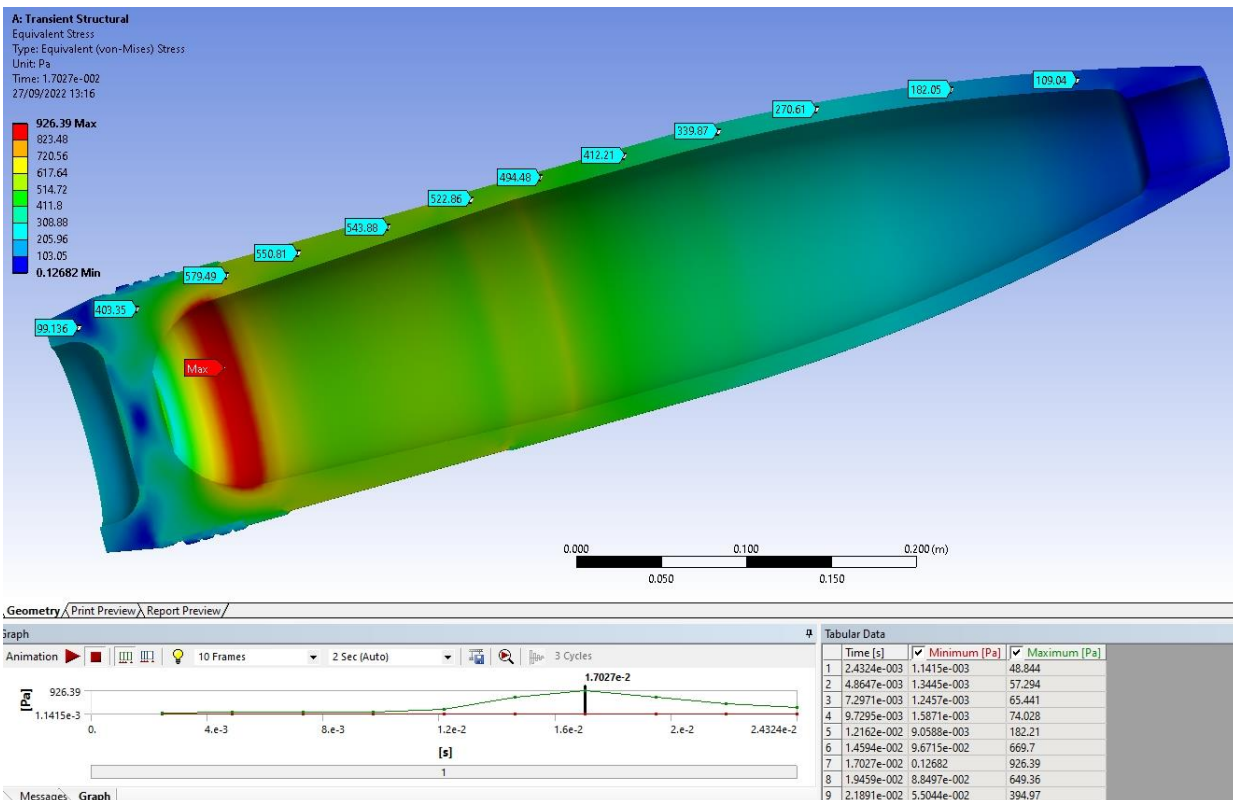


Fig. 16 Equivalent stresses for body of projectile 155mm HE M795

Fig. 17 shows equivalent stresses for 155mm HE M795 projectile, with the explosive charge present. As can be seen, equivalent stresses on explosive charge are lower than 100 MPa.

Fig. 18 shows equivalent stresses for 155mm HE M795 projectile on the outer part of the projectile body. Moving towards the end of the projectile, the equivalent stresses increase up to the location of rotating band. It can also be noticed from Fig. 18 that in the base part of a projectile (hollow base boat tail) equivalent stresses decrease significantly.

This type of numerical analysis can be performed on any type of fast-moving projectile inside the weapon barrel, depending on initial conditions, loads, and geometrical constraints. It is beneficial since it doesn't involve much resources and time and gives very useful data. The limitations of this

approach are in choosing the right material data in numerical simulations, as well as experimental confirmation (verification) of obtained data.

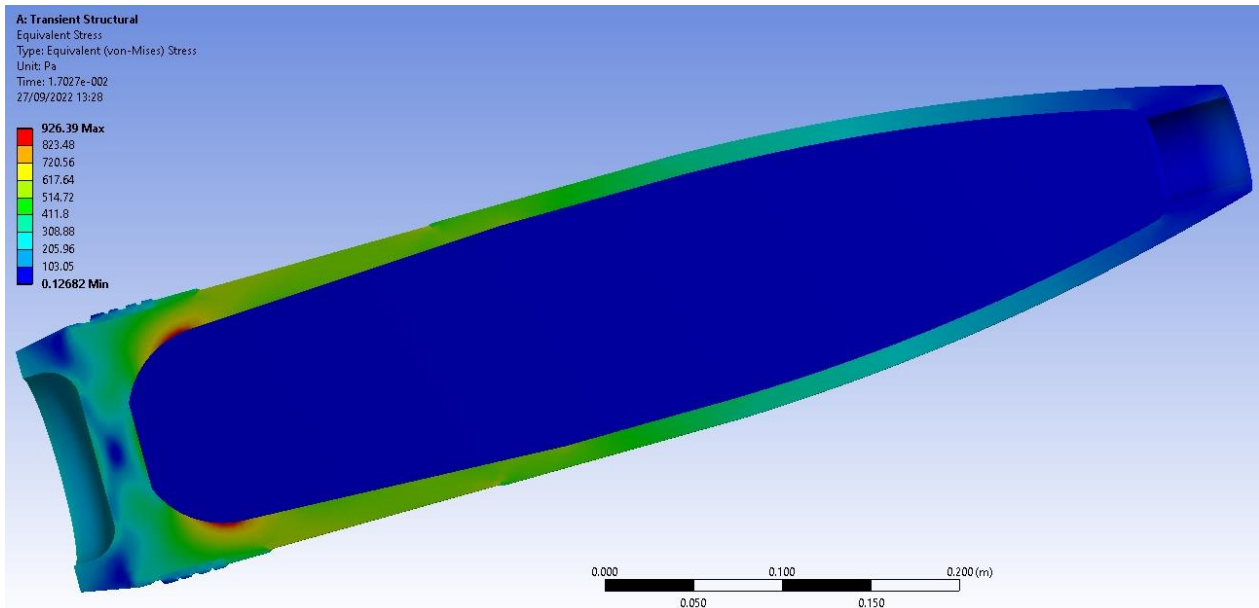


Fig. 17 Equivalent stresses for 155mm HE M795 projectile (all components)

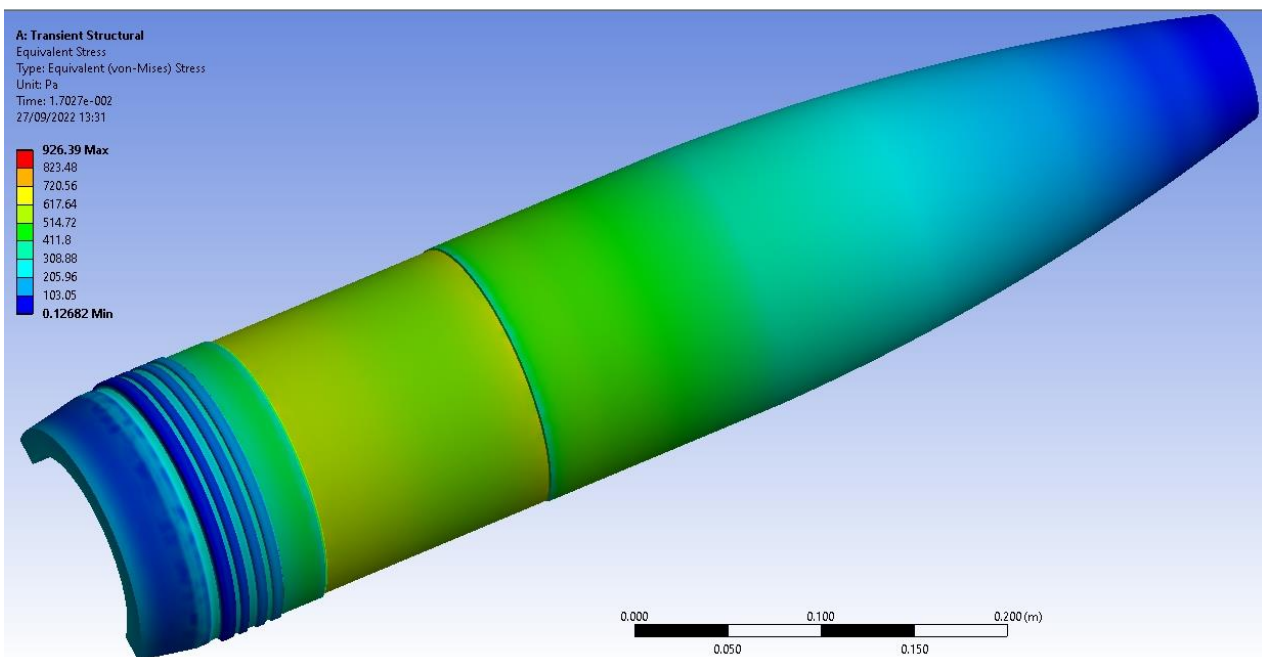


Fig. 18 Equivalent stresses for 155mm HE M795 on the outer part of projectile body

## 5. Conclusions

An overview of research related to the stress state of artillery projectiles during the launch phase is given. The publicly available characteristics of the projectiles 155mm HERA M549 and 155mm HE M795 are presented. Numerical simulations were performed with the 155mm artillery projectiles to determine the maximum equivalent stresses occurring during the launch phase. The obtained values were compared with the yield limit of the materials of the projectile components, in order to assess whether the plastic deformation would potentially occur during the launch phase.

For both projectiles, results show that no plastic deformation occurs during the launch event though base pressures values, obtained using interior ballistics data, were increased by 20% (for in-bore safety measures). The critical section is shown to be section below the rotating band for both projectiles, a result which is in accordance with the conclusions of other authors [18].

Future research could be focused on introduction of projectile rotation in the model and rotating band engraving force. Further phases of the research could also include the use of explicit dynamic codes with the aim of more fully characterizing the phenomena during the launch of ammunition (fluid-solid and solid-solid interaction).

### Declaration of competing interest

The authors state that they do not have any financial or non-financial interests that may influence the content of this paper.

### Funding information

This research was performed without financial support from any funding organization.

## 6. References

- [1] D. E. Carlucci, S. S. Jacobson, *Ballistics - Theory and design of guns and ammunition*, CRC Press, 2018.
- [2] H. Krier, M. Summerfield, *Interior ballistics of guns*, *Progress in Astronautics and Aeronautics - Vol 66*, American Institute of Aeronautics & Astronautics, May 31, 1979.
- [3] *Interior ballistics of guns - Engineering design handbook*, AMCP 706-150, U.S. Army Material Command, February 1965.
- [4] *Army ammunition data sheets artillery ammunition guns, howitzers, mortars, recoilless rifles, grenade launchers and artillery fuzes*, TM 43-0001-28, Headquarters Department of the U.S. Army, Washington, 27 October 2003.
- [5] *Manufacture of projectiles, projectile components, and cartridge cases for artillery, tank main armament, and mortars*, MIL-HDBK-756(AR), 29 April 1991.
- [6] M. R. Brady, P. Goethals, "A comparative analysis of contemporary 155mm artillery projectiles", *Journal of Defense Analytics and Logistics*, vol 3, No. 2, 2019.
- [7] E. L. Baker, M. W. Sharp, "Gun launch and setback actuators", *2018 Insensitive Munitions & Energetic Materials Technology Symposium Portland, OR*, 2018.
- [8] S. Swaszek, E. Baker, "Energetics and munition suitability for gun launch", Picatinny Arsenal, NJ. Available at: <https://imemg.org/wp-content/uploads/2019/11/22229-Paper-Energetics-and-Munitions-Suitability-for-Gun-Launch.pdf>
- [9] D. V. Djurdjevac, *Analysis of stresses for artillery projectile body*, Master Thesis, University of Belgrade, Mechanical Engineering Faculty, 2008.
- [10] V. Tanguay, *Parametric study on the interior ballistics of 105mm and 155mm artillery guns*, DRDC Valcartier, TM 2007-350, March, 2008.
- [11] G. Herder, F. P. Weterings, W. P. C. de Klerk, "Mechanical analysis on rocket propellants", *Journal of Thermal Analysis and Calorimetry*, Vol. 72, pp 921-929, 2003.
- [12] J. Pinto, D. A. Wiegand, *Yield and plastic flow in composition B and TNT*, U.S. Army Armament Research, Development and Engineering Center, Picatinny Arsenal, New Jersey, January 1993.
- [13] L. Stiefel, *Gun propulsion technology*, *Progress in Astronautics and Aeronautics - Vol. 109*, American Institute of Aeronautics & Astronautics, 1998.
- [14] Ansys - Help Manuals, Ansys Inc, [www.ansys.com](http://www.ansys.com).
- [15] *Structural Analysis Guide*, Ansys Inc., April 2009.
- [16] <https://www.gd-ots.com/>
- [17] <https://www.globalsecurity.org/military/systems/munitions/m795.htm>
- [18] J. H. Mulherin, W. B. Steward, J. D. Corrie, *Fracture mechanics study on 155 mm M107e1 projectile made from isothermally transformed HF-1 steel*, U.S. ARMY Armament Command, Frankford Arsenal, Philadelphia, Pennsylvania, 1976.

- 
- [19] Barton, 155mm M795 Aerofuze test at the Kofa range, Yuma Proving Ground, Arizona, 19 May 2015.
- [20] C. Taylor, J. Starkenberg, L. H. Ervin, An experimental investigation of Composition-B ignition under artillery setback conditions, US Army ARDEC BRL, Aberdeen Proving Ground, Maryland, 1980.
- [21] L. W. Burton, C. P. R. Hoppel, R. P. Kaste, Feasibility of a 7,000-lb 155-mm towed howitzer, Army Research Laboratory, 1996.
- [22] R. W. Collett, "Measurement of in-bore set-back pressure on projectile warheads using hard-wire telemetry", *International Telemetry Conference Proceedings*, 1983.
- [23] H. Babaei, M. Malakzadeh, H. Asgari, "Stress analysis of gun barrel subjected to dynamic pressure", *International Journal of Mechanical Engineering and Applications*, Vol. 3, pp 71-80, 2015.
- [24] M. Ervin, A. Di Stasio, "U. S. Army common low-cost insensitive munition program IMX-101 replacement for TNT explosive for 155mm M795 IM projectile", *Joint Armaments Conference*, May 2010.
- [25] S. E. Ray, M. J. Nusca, A. W. Horst, A study of ammunition response to the interior ballistics environment of gun launch, Army High Performance Computing Research Center Minneapolis, 2006.
- [26] M. Liennard, O. Chevalier, A. Langlet, Y. Guilmar, M. Mansion, "An analysis of the accelerations of a projectile in a gun tube by direct measurements and telemetry of the data", *Mechanics & Industry, EDP Sciences*, pp 406, 2018.
- [27] R. Fredriksson, V. Hellberg, Calculation of fluid dynamic loads on a projectile during firing, Master Thesis, Linköpings universitet, 2016.
- [28] S. Wilkerson, D. Hopkins, G. Gazonas, M. Berman, Developing a transient finite element model to simulate the launch environment of the 155-mm SADARM projectile, Army Research Laboratory, 2000.
- [29] J. M. Bender, L. E. Reinhardt, A Comparison of structural analysis techniques for the Excalibur 155-mm artillery shell's canard actuation system, ARL-TR-3409, 2005.
- [30] P. Verberne, S. A. Meguid, "Dynamics of precision guided projectile launch: solid-solid interaction", *International Journal of Structural Stability and Dynamics*, 2020.
- [31] R. H. Dohrn, D. E. Carlucci, J. F. Newill, Gun launch dynamics - benchmarking the state of the art, Army Research Laboratory, April 2011.
- [32] M. M. Chen, Launch survivability analysis of on-board components of the Extended Area Protection and Survivability (EAPS) projectile system, ARL-TR-4484, 2008.
- [33] J. Cordes, J. Vega, D. Carlucci, Structural loading statistics of live gun firings for the Army's Excalibur projectile, Technical Report ARAET-TR-05005, 2005.
- [34] R. Lee, Instrumented projectile firings in a 155-mm Regenerative Liquid Propellant Gun (RLPG) system, Technical ARFSD-TR-93039, Army Armament Research, Development and Engineering Center, Picatinny Arsenal, NJ, November, 1993.
- [35] D. W. Lodge, A. M. Dilkes, Use of an instrumented 120mm projectile for obtaining in-bore gun dynamics data, Defense Evaluation and Research Agency Surrey (United Kingdom), April, 2001.
- [36] S. A. Wilkerson, M. Palathingal, Analysis of an instrumented projectile, Technical Report ARLMR-383, Army Research Lab Aberdeen Proving Ground MD, ADA335770, December, 1997.
- [37] B. S. David, T. G. Brown, C. R. Myers, M. S. Hollis, Ground and flight testing of microelectromechanical systems sensors for the commercial technology insertion program, Army Research Lab, Aberdeen Proving Ground, MD, Sep, 1997.
- [38] G. L. Katulka, P. J. Peregino, P. C. Muller, K. McMullen, R. Wert, In-bore ballistic measurements with wireless telemetry in kinetic energy electro-thermal-chemical projectiles, U.S. Army Research Laboratory, Aberdeen Proving Ground, MD, September 2003.
-

- [39] E. A. Szymanski, Acquiring data for the development of a finite element model of an airgun launch environment, U.S. Army Research Laboratory, Aberdeen Proving Ground, MD, 19 May, 2004.
- [40] R. E. Ball, Survivability of the 127mm gun-launched finned motor case, AD-754 378, 1972.
- [41] P. Verberne, Multiphysics modelling of the coupled behaviour of precision-guided projectiles subjected to intense shock loads, Master Thesis, Department of Mechanical and Industrial Engineering, University of Toronto, 2014.
- [42] J. A. Cordes, D. E. Carlucci, J. Kalinowski, L. Reinhardt, Design and development of reliable gun-fired structures, Technical Report ARAET-TR-06009, ARDEC, Picatinny Arsenal, New Jersey, 2006.
- [43] J. A. Cordes, P. Vo, J. R. Lea, D. W. Geissler, J. D. Metz, D. C. Troast, A. L. Totten, "Comparison of shock response spectrum for different gun tests", *Shock and Vibration*, Vol. 20, pp 481-491, 2013.
- [44] R. D. Anderson, K. Fickie, IBHVG2 - A User's Guide, Technical Report BRL-TR-2829, US Army Ballistic Research Laboratory, Aberdeen Proving Ground, Maryland, 1987.
- [45] V. Chakka, M. B. Trabia, B. O'Toole, S. Sridharala, S. Ladkany, M. Chowdhury, Modeling and reduction of shocks on electronic components within a projectile, Army Research Laboratory, ARL-RP-217, Adelphi, MD, August 2008.
- [46] J. E. Alexander, "Advanced gun system gun and projectile dynamic model results and correlation to test data", *Journal of Pressure Vessel Technology*, Vol. 134, August 2012.
- [47] E. Petersen, "AGS barrel motion during firing: experimental and modeling results", *Proceedings of the 2005 SEM annual conference and exposition on experimental and applied mechanics, Society for Experimental Mechanics*, Bethel, CT, 2005.
- [48] [https://www.mm.bme.hu/~gyebro/files/ans\\_help\\_v182/ans\\_thry/thy\\_anproc2.html](https://www.mm.bme.hu/~gyebro/files/ans_help_v182/ans_thry/thy_anproc2.html)